Biomechanical comparisons of different diagonal screw designs in a novel embedded calcaneal slide plate

Shun-Ping Wang[a,b,c], Wei-Yi Lai[d], Yi-Yin Lin[d], Tzu-Wei Lin[d], Ming-Tzu Tsai[e], Yi-Ping Yang[d], Cheng-En Hsu[a,b], Chao-Ping Chen[a,f,g], Cheng-Hung Lee[a,c,h], Kuo-Chih Su[e,i,j,*]

[a]Department of Orthopedics, Taichung Veterans General Hospital, Taichung, Taiwan, ROC; [b]Sports Recreation and Health Management Continuing Studies-Bachelor's Degree Completion Program, Tunghai University, Taichung, Taiwan, ROC; [c]College of Medicine, National Chung Hsing University, Taichung, Taiwan, ROC; [d]Department of Medical Research, Taipei Veterans General Hospital, Taipei, Taiwan, ROC; [e]Department of Biomedical Engineering, Hungkuang University, Taichung, Taiwan, ROC; [f]Department of Health Services Administration, China Medical University, Taichung, Taiwan, ROC; [g]Department of Acupressure Technology, Jen-Teh Junior College of Medicine, Nursing and Management, Miaoli, Taiwan, ROC; [h]Department of Food Science and Technology, Hungkuang University, Taichung, Taiwan, ROC; [i]Department of Medical Research, Taichung Veterans General Hospital, Taichung, Taiwan, ROC; [j]Department of Chemical and Materials Engineering, Tunghai University, Taichung, Taiwan, ROC

Abstract

Background: Medial displacement calcaneal osteotomy (MDCO) is frequently used for the surgical correction of flatfoot. This study aims to investigate the biomechanical effect of the different diagonal screw design on a novel-designed embedded calcaneal plate for MDCO using finite element analysis (FEA), mechanical test and digital image correlation (DIC) measurement.

Methods: Four groups according to the varied implanted plate were set as control group (Group 1), non-diagonal screw (Group 2), one-diagonal screw (Group 3), and two-diagonal screws groups (Group 4). For FEA, A 450 N load was applied to on the anterior process of the calcaneus from top to bottom. Observational indices included the stress on the cortical and cancellous bone of the calcaneus surrounding the implant, the plate itself as well as screws, and the displacement of the overall structure. In addition, this study also used in vitro biomechanics test to investigate the stiffness of the structure after implantation, and used DIC to observe the displacement of the calcaneus structure after external force.

Results: Under a simulated load in FEA, there are significant overall instability and high stress concentration on the calcaneal surrounding host bone and the plate/screws system, respectively, in group 2 compared with other groups. Regard to the mechanical testing with DIC system, significant increased rotation stability, maximum force and stiffness with the addition of diagonal screws. In comparison to Group 2, the increase of 112% and 157% in maximum force as well as 104% and 176% in stiffness were found in Group 3 and 4, respectively.

Conclusion: For reducing stress concentration and enhancing overall stability, more than one-diagonal screw design is recommended and two-diagonal screws design will be superior. This study provided biomechanical references for further calcaneal implants design to prevent clinical failure after MDCO.

Keywords: Digital image correlation; Embedded calcaneal slide plate; Finite element analysis; Medial displacement calcaneal osteotomy

1. INTRODUCTION

Adult acquired flatfoot deformity (AAFD) is a common foot problem in adults[1] that can cause foot deformity and pain, and affect walking and quality of life.[2,3] The prevalence of symptomatic stage II AAFD is about 3.3%[4] and surgical reconstruction is often necessary if conservative treatment fails.[5,6] Common surgical corrective treatments include medial displacement calcaneal osteotomy (MDCO) and other soft tissue reconstruction surgeries.[6,7] Although there is no consensus on surgical methods for type II AAFD, MDCO is a widely used bony procedure to correct AAFD.[8] MDCO can correct the hindfoot alignment, promote the success rate of soft tissue reconstruction, and improve the mechanical distribution of the foot,[9,10] thereby achieving good therapeutic efficacy and patient satisfaction.[11,12]

MDCO can be fixed by internal fixation using screws or a lateral bone plate to promote bony union.[8,13,14] However, screw fixation can cause a number of surgical complications, including posterior heel pain, hardware irritation, infection and difficulty in wearing shoes. The complication rate ranges from 29% to 47% and which increases the number of operations, surgical risks, and medical costs.[13,15,16] Therefore, fixed-angle lateral calcaneal slide plates became started to be used for MDCO in recent

*Address correspondence. Dr Kuo-Chih Su, Department of Medical Research, Taichung Veterans General Hospital, 1650, Taiwan Boulevard Section 4, Taichung 407, Taiwan, ROC. E-mail address: kcsu@vghtc.gov.tw; kaoche2000@gmail.com (K.-C. Su).

Conflicts of interest: The authors declare that they have no conflicts of interest related to the subject matter or materials discussed in this article.

Journal of Chinese Medical Association. (2021) 84: 1038-1047.

Received August 4, 2021; accepted September 13, 2021.

doi: 10.1097/JCMA.0000000000000625.

years due to the advantages of less hardware complications[15] and better stability compared to screw fixation.[17]

Currently, a number of different calcaneal slide plate designs exist. Some are attached to the lateral calcaneus by screws fixation, and some are designed to insert the embedded blade into the proximal calcaneus for fixation. These new-generation calcaneal bone plates with embedded design significantly reduce the removal rate range from 1.05% to –1.6% caused by symptomatic hardware[15,18–20] and can supply a good model of novel design on calcaneal slide plate for MDCO. Up to our knowledge, there is still paucity of biomechanical studies on those embedded calcaneal plates used after MDCO.

Finite element analysis (FEA) applied on calcaneal fractures in previous biomechanical studies[21–23] is also appropriate to investigate the stability, stress distribution, and displacement after implantation for MDCO in this study. The FEA is helpful to evaluate the stress concentration or strain distribution at implants and surrounding host bone. Digital image correlation (DIC) is a useful technique to provide 3D evaluation of displacement and strain.[24] The biomechanical test combined with DIC measurement offers the data about the required load to translation and rotation for further assessing the linear and rotation stability of the tested specimen. Furthermore, 3D printing offers the potential advantages of cost-benefit for manufacturing and designing implants in surgeries of foot and ankle procedures. The preclinical evaluation including finite element, biomechanical test, and DIC measurement used in the current study for the stability of newly designed implants is important to prevent clinical failures.

Notably, the diverse diagonal screw structures have been designed on those newly designed embedded calcaneal slide plates. However, their biomechanical property after implantation is still not clear and should be further studied to prevent clinical failures. Before investigating the effect of diagonal screws fixation on the embedded bone plates, a new calcaneal slide plate was specially designed and manufactured by 3D printing in the experiment for MDCO first. This study aimed to investigate the biomechanical effects of different diagonal screw settings on the embedded bone plates and the cortical and cancellous host bone surrounding the implant using FEA and biomechanical test. The hypothesis of this study is that more than one-diagonal screw can provide adequate stability and lower stress on implant and surrounding bone. The results of this study are able to provide orthopedic surgeons and researchers the further understanding of the biomechanical effect of different designs of the embedded calcaneal slide plate after implantation.

2. METHODS

In order to investigate the biomechanical effects of different diagonal screw on the novel embedded calcaneal slide plate, FEA、DIC measurement and biomechanical test were used to evaluate the stability and the biomechanical effect of the diagonal screw on the novel calcaneal slide plate.

2.1. MDCO and novel embedded calcaneal sliding plate

MDCO is performed through the lateral wall of the calcaneus. An oscillating saw is used to cut along the long axes of the calcaneal tuberosity, and the sawed calcaneal tuberosity is displaced medially by 8–10 mm[8]. In this study, a novel embedded calcaneal slide plate was specially designed. The overall structure of this bone plate includes head and connecting bridge of the plate, an embedded tapered blade tail, fixation screws, and diagonal screws (Fig. 1A). The main features of this bone plate are: (1) The preset displacement distance on this plate for moving osteotomy about 8–10 mm that thus facilitate surgical conveniences for surgeons.

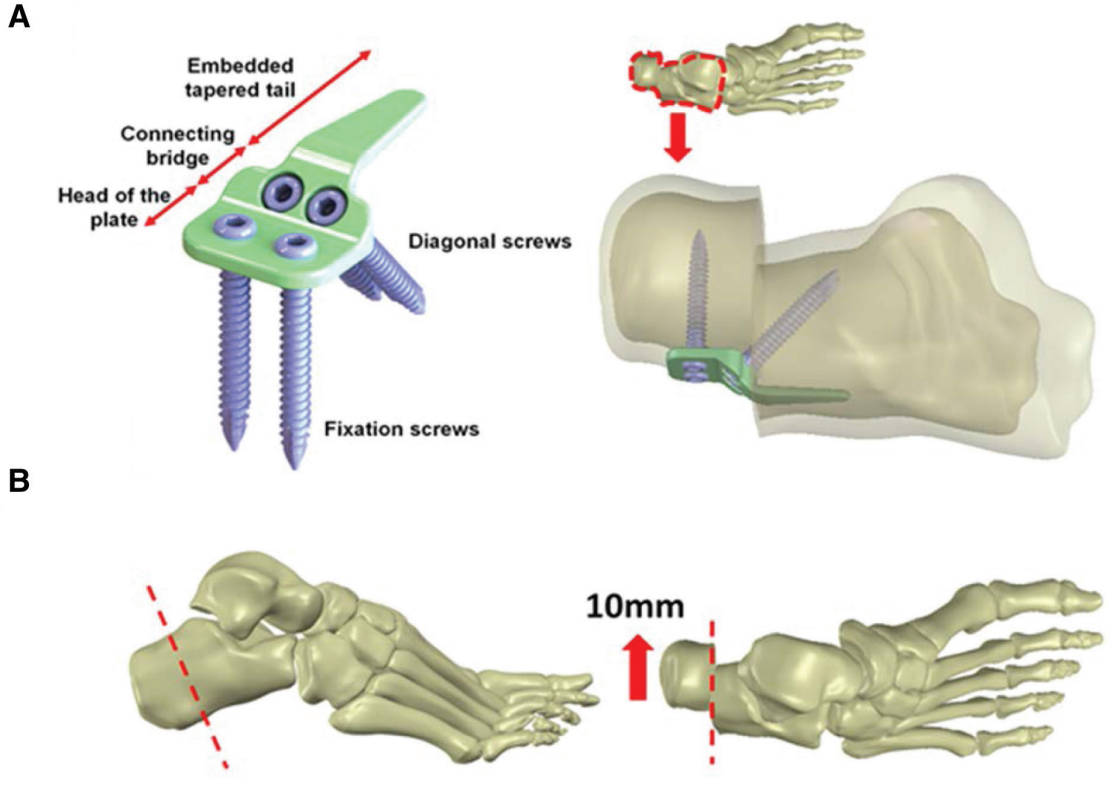

Fig. 1 Calcaneal slide plate and MDCO surgery. A, Using the novel embedded calcaneal slide plate for fixation in the present study. B, MDCO, the calcaneus parallel to the axis of the tuberosity and shift it 10 mm. MDCO = medial displacement calcaneal osteotomy.

(2) A tapered tail blade of this plate can be completely embedded in the proximal calcaneus to avoid hardware irritation. (3) Diagonal screws are designed at the connecting bridge to increase the stability of the implant, increase the proximity between the calcaneal bone blocks, and promote bone healing.

2.2. Building a simulation geometry model

In order to use FEA to investigate a novel embedded calcaneal slide plate, a finite element computer model of the calcaneus with the novel embedded calcaneal slide plate implanted was constructed. The structures in the computer model used in this study consisted primarily of five parts: the cortical and cancellous bone of the calcaneus, the novel embedded calcaneal slide plate, the fixation screws, and the diagonal compression screws. The model of the calcaneus was constructed using computerized tomography (CT) images from the Visible Human Project of the National Institutes of Health. The Mimics medical image reconstruction software (Mimics Medical 20.0; Materialise, Leuven, Belgium) was used on the CT images to reconstruct the segmentation of the human calcaneus (Fig. 1B), and the CT image grayscale values were used to distinguish cortical bone from the cancellous bone. Accordingly, the calcaneus model constructed in this study is divided into two parts: cortical bone and cancellous bone. Three-dimensional computer-aided design (CAD) software (Solidworks 2016, Dassault Systemes SolidWorks Corp, Waltham, MA, USA) was used to create a model of the novel embedded calcaneal slide plate. In addition, in order to simulate the tuberosity of the sawn calcaneus during MDCO, the tuberosity of the calcaneus was displaced 10 mm medially, and the CAD software was used to cut the calcaneus parallel to the axis of the tuberosity and shift it 10 mm (Fig. 1B), simulating the implantation of the novel embedded calcaneal slide plate to fix the bone after MDCO. The study investigated the impact of diagonal screw implantation on the plate and bone in different situations. Therefore, four different settings (Fig. 2) were constructed (intact calcaneus without plate fixation and non-diagonal screw, one-diagonal screw, or two-diagonal screws on connecting bridge of the implanted plate, respectively). After constructing the 3D computer model of the calcaneus implanted with the novel embedded calcaneal slide plate, the model was imported into the ANSYS Workbench FEA software (version 18.0, ANSYS, Inc., Canonsburg, PA, USA) for FEA. The first group (Group 1) was set as the control group with an intact calcaneal structure. After simulated calcaneal osteotomy for MDCO in FEA, the other experimental modules were implanted with the embedded calcaneal plate with fixation screws (located at s1 and s2) as well as non-diagonal screws, one-diagonal screw (located at s3), and two-diagonal screws (located at s4 and s5) in Group 2, Group 3, and Group 4, respectively.

2.3. Loading conditions and boundary conditions

This study investigated the biomechanical effects of different designs of the novel embedded calcaneal slide plate. In the FEA, different loading conditions and boundary conditions were entered based on settings from previous studies.[23] When setting the loading conditions in the present study, a downward force of 450 N was applied to the anterior process of the calcaneus (Fig. 3). When setting the boundary conditions, the calcaneal tuberosity was set as a fixed end, and the X-axis, Y-axis, and Z-axis displacement was set to 0. In addition, for MDCO, the contact between the open sections was set to "no separation" type; the main purpose was to simulate a cut that allowed for slight frictionless sliding.[22]

2.4. Material properties of the model

The FEA model in this study was composed of five parts, namely the cortical and cancellous bone of the calcaneus, the novel embedded calcaneal slide plate, the fixation screws, and the diagonal compression screws. The properties of the materials used in this study are mentioned in previous studies.[19,23]

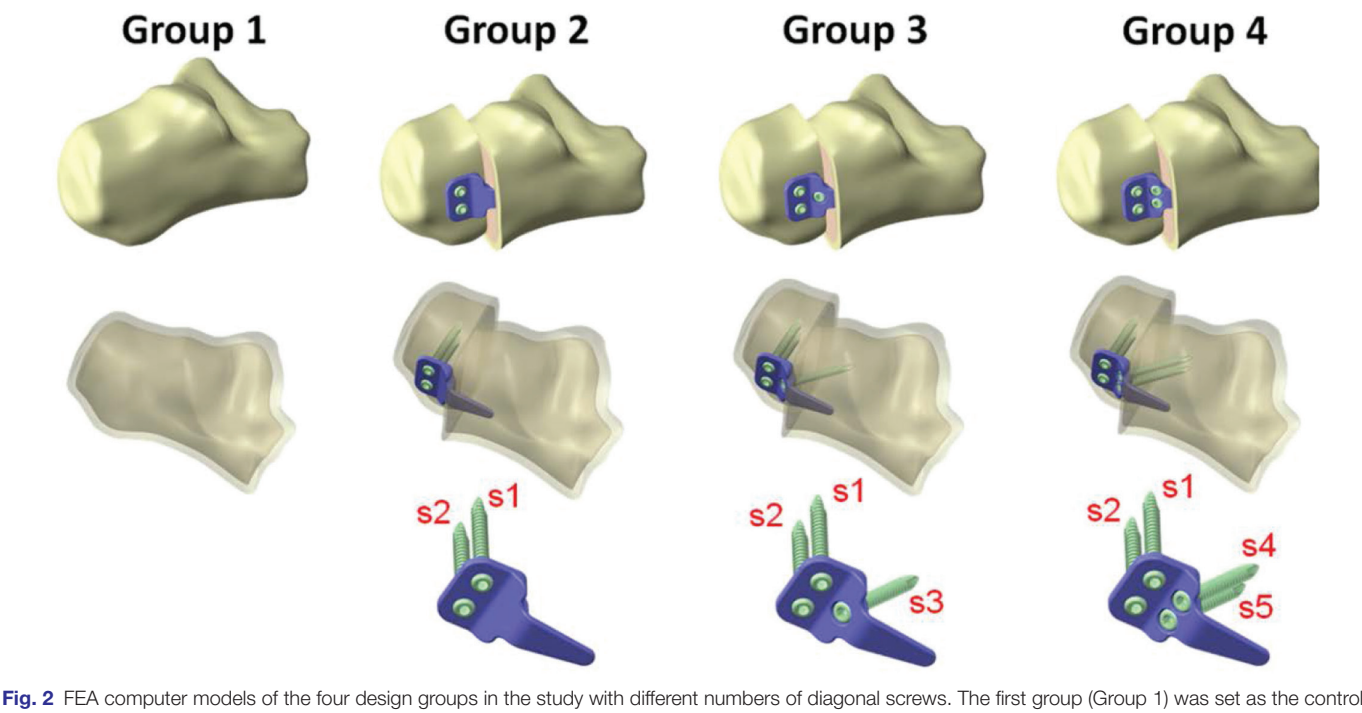

Fig. 2 FEA computer models of the four design groups in the study with different numbers of diagonal screws. The first group (Group 1) was set as the control group with an intact calcaneal structure. After simulated calcaneal osteotomy for MDCO in FEA, the other experimental modules were implanted with the embedded calcaneal plate with fixation screws (located at s1 and s2) as well as no-diagonal screws, one-diagonal screw (located at s3) and two-diagonal screws (located at s4 and s5) in Group 2, Group 3, and Group 4, respectively. FEA = finite element analysis; MDCO = medial displacement calcaneal osteotomy.

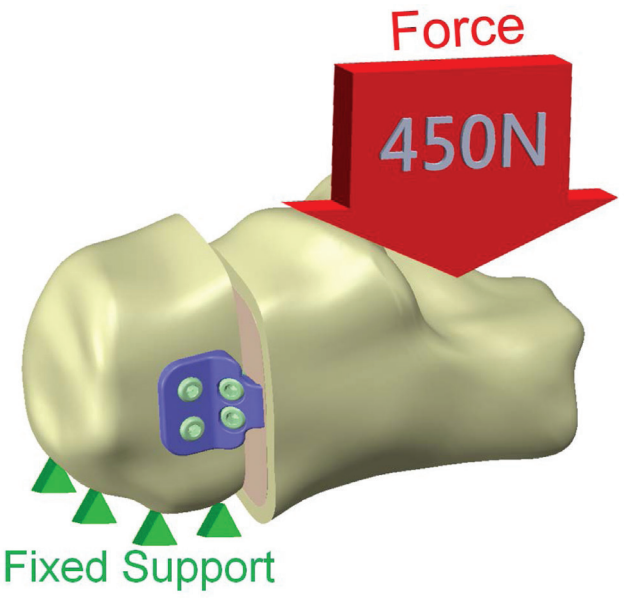

Fig. 3 Loading conditions and boundary conditions.

Table 1 shows the material properties used in the simulation of this study. All materials were assumed to be homogeneous, isotropic, and linearly elastic. Therefore, two independent parameters (Young's modulus [E] and Poisson's ratio [v]) were used to express the material properties. In addition, the mesh elements used in the FEA computer model in this study was a tetrahedral mesh (Fig. 4). After convergence testing of the mesh, the size of the mesh was 1 mm, and the model reached 5% of the stop criterion of the convergence test.[21] The number of nodes and elements used in each group of FEA computer models is shown in Figure 4.

After FEA, the von Mises stress distribution diagram was used as the observation index (von Mises stress is $\sigma_{von} = \sqrt{\frac{1}{2}\left[(\sigma_1 - \sigma_2)^2 + (\sigma_1 - \sigma_3)^2 + (\sigma_2 - \sigma_3)^2\right]}$), where σ1, σ2, and σ3 are the principal stresses in the three axial directions. The main observational indices are the stress on the cortical bone of the calcaneus, the cancellous bone of the calcaneus, the novel embedded calcaneal slide plate, the fixation screws, the diagonal compression screws, and the displacement of the overall structure.

2.5. Preparation of the specimen for in vitro biomechanics test

The synthetic calcaneus (9147; SYNBONE, Zizers, Switzerland) was used as bone model in this study. Synthetic bone models were popularly used in the preclinical testing with the advantages of homogeneity to reduce the inter-specimen variability. The calcaneal osteotomy was made perpendicular to the long axis of each synthetic calcaneus at 20 mm anterior to the apex of calcaneal tuberosity. The tested newly designed calcaneal plates for MDCO fixation in this study were printed by 3D printer (Form 3; Formlabs, Somerville, MA, USA) using rigid material. Those tested bone plate were made as the desired designs of diagonal screws in different experimental groups and then they were implanted to the osteotomized calcaneus for MDCO fixation with 10 mm medial displacement.

Table 1

Settings of the material properties in this study

Materials	Young's modulus (MPa)	Poisson's ratio
Cortical bone	7300	0.3
Cancellous bone	100	0.3
Titanium	110 000	0.3

2.6. Biomechanical test and load configuration

In order to mechanical test, a reliable frame for fixation of the implanted calcaneus was adopted. To compare the mechanical stability of the different designed bone plate, four groups were set as control group with normal calcaneus, and the other three experimental groups fixed by calcaneal slide plates with non-diagonal screw, one-diagonal screw, or two-diagonal screws, respectively (Fig. 5A). After well stabilizing the tested modules on the frame of material testing system (JSV-H1000; Japan Instrumentation System, Nara, Japan), the loads were transmitted by a steel wedge on the anterior process of the experimental calcaneus from top to bottom to allow for downward translation of the implanted calcaneal modules. The implants were not loaded to failure because the clinical implant failure often caused by submaximal impacts after a high number of cycles. Five separated tests were performed for each bone modules. The increasing loads to displace the tested modules every 0.1 mm inferiorly until to 1.0 mm were recorded to evaluate the stiffness of these modules and the maximum force required to achieve 1.0 mm downward translation of the tested modules. In order to evaluate the rotation instability of the experimental modules, the commercial digital image correlation (DIC) system (VIC, Correlated Solutions Inc., Irmo, SC, USA) was used (Fig. 5B). The surfaces of the studied specimens were painted with a black-on-white speckle pattern for DIC software (Vic-2D Digital Image Correlation Version 6.0.2, Correlated Solutions Inc.) to correlate and track it properly. The DIC measurements were based on optical system to capture the speckle painted image on the bone surface by two different digital cameras. As the load applied from top on the anterior synthetic implanted calcaneus, the rotation deformation on the front bone surface over the area of interest was recorded during the loading process and further analyzed with the DIC software.

2.7. Statistical analysis

The maximum force and stiffness of the four fixation constructions were analyzed using Kruskal-Wallis test and post hoc analysis by Bonferroni test with a 0.05 level of significance. All statistical analyses were performed using the Statistical Package for the Social Science (IBM SPSS version 22.0; International Business Machines Corp, Armonk, NY, USA).

3. RESULTS

The stress distribution of the embedded calcaneal slide plate and the overall structure of the calcaneus was obtained through FEA. The distribution of von Mises stress on the calcaneal cortical bone without any implant (Group 1) and with implants in the other 3 groups using novel embedded calcaneal slide plates with different diagonal screws design was shown in Fig. 6A. Of these, Group 2 had highest stress on the cortical bone surface. In addition, the stress in the area of the embedded calcaneal slide plate and the fixation screws did not greatly differ among the groups (Group 2, Group 3, and Group 4), and the stress near the fixation screws was low.

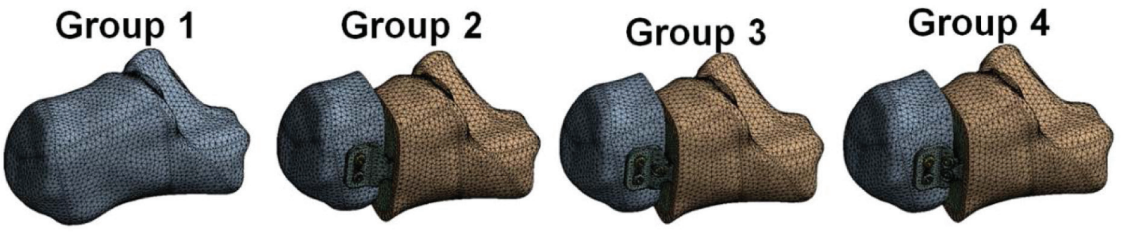

Mesh number	Group 1	Group 2	Group 3	Group 4
Nodes	92,241	266,888	347,938	419,674
Elements	52,642	155,743	203,817	246,282

Fig. 4 Computer model meshes used and the number of nodes and elements in the study.

Fig. 6B shows the stress distribution on the cross-section of calcaneal cancellous bone of the four groups. The figure shows that Group 2 had highest stress at the protruding insertion point near the embedded tapered blade tail of the bone plate. In Groups 3 and 4, there was high stress distributed on the diagonal compression screws, especially on the screw threads, but most of the stress values were less than 10 MPa.

Fig. 6C shows the stress distribution of the embedded calcaneal slide plate on the cancellous bone. The figure also shows that Group 2 has higher stress at the protruding insertion point near the embedded tapered blade tail of the bone plate. Table 2 shows the maximum von Mises stress values on the cancellous bone of the diagonal screws in the implanted embedded calcaneal slide plate. The results show that the maximum stress value is located at the bone near the diagonal screws in Group 3. The stress value on the bone near the diagonal screw in Group 4 is half of that in Group 3.

Fig. 7A shows the von Mises stress distribution on the embedded calcaneal slide plate. In Group 2, there is highest stress produced on the protruding insertion point near the embedded tapered blade tail of the bone plate.

Fig. 7B shows the von Mises stress distribution on the fixation screws and diagonal screws of the embedded calcaneal slide plate system. Fig. 7B shows that there is little difference in the stress distribution on the fixation screws among the groups, but there is obvious high stress on the diagonal screw in Group 3. Table 3 shows the maximum von Mises stress values on the fixation screws and diagonal screws of the embedded calcaneal slide plate system.

Fig. 8A shows the overall structural displacement of each group after loaded with an external force and Group 2 experienced a largest displacement. In addition, the displacement distribution of Groups 3 and 4 are similar, but the maximum displacement of Group 3 is greater than that of Group 4 by about 0.6 mm. Fig. 8B shows the direction of displacement in each group.

According to the experimental data of the biomechanical test, the median of maximum force to downward translation of the studied calcaneal modules were 27.56, 4.12, 8.73, and 10.59 N and the stiffness were 24.27, 3.34, 6.81, and 9.21 N/mm in control, non-, one-, and two-diagonal screw groups, respectively (Table 4). The maximum force and stiffness in

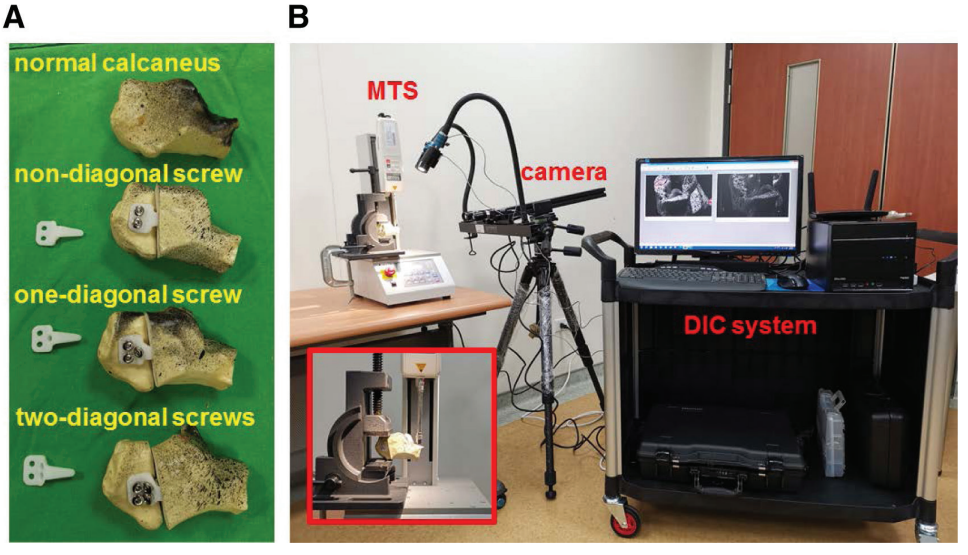

Fig. 5 Biomechanical test. A, Four groups were set as control group with normal calcaneus, and the experimental specimens in other three groups fixed by calcaneal slide plates with non-diagonal screw, one-diagonal screw, or two-diagonal screws, respectively. B, Experimental setup for in vitro biomechanical testing with DIC system. DIC = digital image correlation; MTS = material testing system.

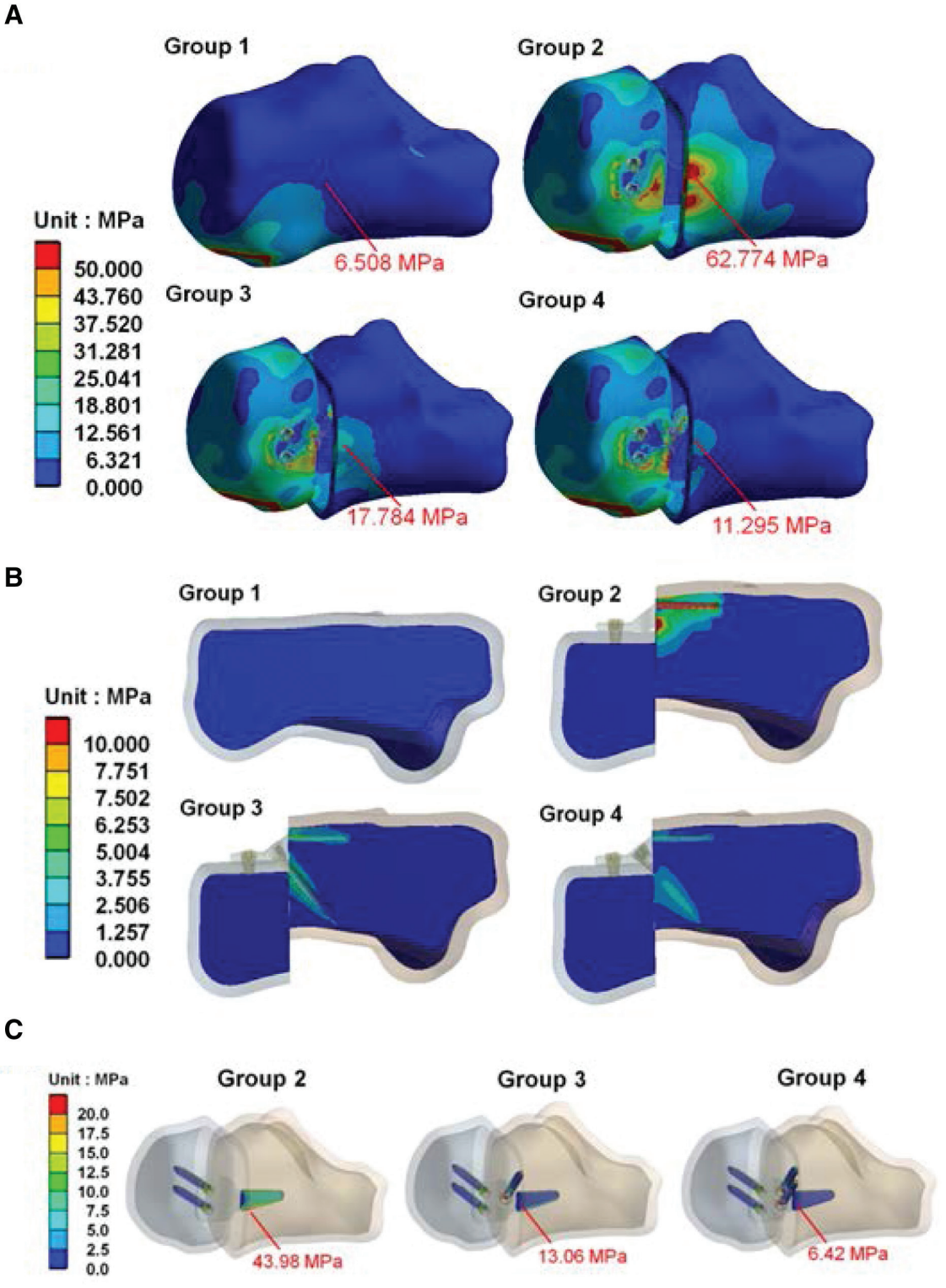

Fig. 6 von Mises stress distribution on the calcaneus. A, Distribution of von Mises stress on the calcaneal cortical bone in each group. B, Distribution of von Mises stress on the cross-section of calcaneal cancellous bone in each group. C, Stress distribution of the embedded calcaneal slide plate system on the cancellous bone.

one-diagonal screw and two-diagonal groups were significant higher in comparison to those of non-diagonal group by increase of 112% and 157% in maximum force as well as 104% and 176% in stiffness. Notably, there were no significant differences between one-diagonal screw and two-diagonal groups regard to maximum force and stiffness, according to Kruskal-Wallis test (Fig. 9).

After analyzed by the specialized software for DIC measurement, the deformation of speckle paints from the DIC measurements on front surface of the experimental calcaneal

Table 2

Maximum von Mises stress of the upper screw of the embedded calcaneal slide plate system on the cancellous bone

Bone	s1	s2	s3	s4	s5
Group 2	118.60 MPa	100.13 MPa	—	—	—
Group 3	137.03 MPa	100.44 MPa	690.22 MPa	—	—
Group 4	130.96 MPa	95.40 MPa	—	348.60 MPa	293.03 MPa

—, not available.

modules elucidated the downward translation associated with load progression from the top of specimens in all groups and the obvious rotational instability happened in the non-diagonal screw group. The rotation stability in two-diagonal screws group was better than one of one-diagonal screw group (Fig. 10).

4. DISCUSSION

The present study aimed to use FEA to investigate the biomechanical conditions of the novel embedded calcaneal slide plate after implantation in the calcaneus. The results of the study can provide biomechanical reference to clinical orthopedic surgeons and researchers after implantation of the calcaneal slide plate for MDCO.

The von Mises stress distribution on the calcaneus shows that high stress was found on the cortical and cancellous bone of the calcaneus near the lateral side of the embedded tapered blade tail, especially in Group 2, because the plate fixation in this group only relies on a single tapered blade tail; hence, a relatively high stress is produced. In the other groups (Groups 3 and 4), the force is transmitted not only by the tapered blade tail but also by the diagonal screws used for fixation; therefore, the stress on the calcaneus is reduced. When the number of diagonal screws is increased, the stress on the embedded tapered blade tail on the calcaneal bone can be shared. In addition, low stress with no significant differences among the groups (Groups 2, 3, and 4) over the calcaneal areas at the head part of the novel embedded slide plate where fixation screws were placed, and it may be due to the stress shielding effect.

In addition, the von Mises stress distribution on the embedded calcaneal slide plate shows that when the plate is designed without diagonal screws (Group 2), only the embedded tapered blade tail of the bone plate provides fixation to and is connected to the calcaneus. Therefore, the tapered blade tail of the bone plate experiences higher stress. In addition, the stress on the diagonal screw shows that a higher stress is found at the osteotomized site. However, due to the design of the diagonal screw, the stress on the tapered blade tail of the bone plate is also greatly reduced. Furthermore, when the number of diagonal screws is increased, the stress value on the diagonal screws at the intersection of the osteotomized site was also reduced.

In addition, the displacement of each group was observed in order to evaluate the stability of the different embedded calcaneal slide plate designs. It was found that the displacements of the implanted diagonal screws were similar between Groups 3 and 4 (Fig. 8A), but the displacement in the implant with two-diagonal screws (Group 4) was small. Although the stability in Group 3 or 4 is reduced compared with the case of the calcaneus without implant fixation (Group 1), their stability still more increased than Group 2. In addition, the direction of displacement in each group was also observed (Fig. 8B), and it was found the bone plate without diagonal screws and only relying on the tapered blade tail in Group 2 for fixation makes it more prone to rotation in addition to insufficient stability, which may lead to postoperative failure.

According to the finding of preclinical testing in current study, there was more maximum force for 1.0 mm translation and stiffness in two-diagonal screw group than those in

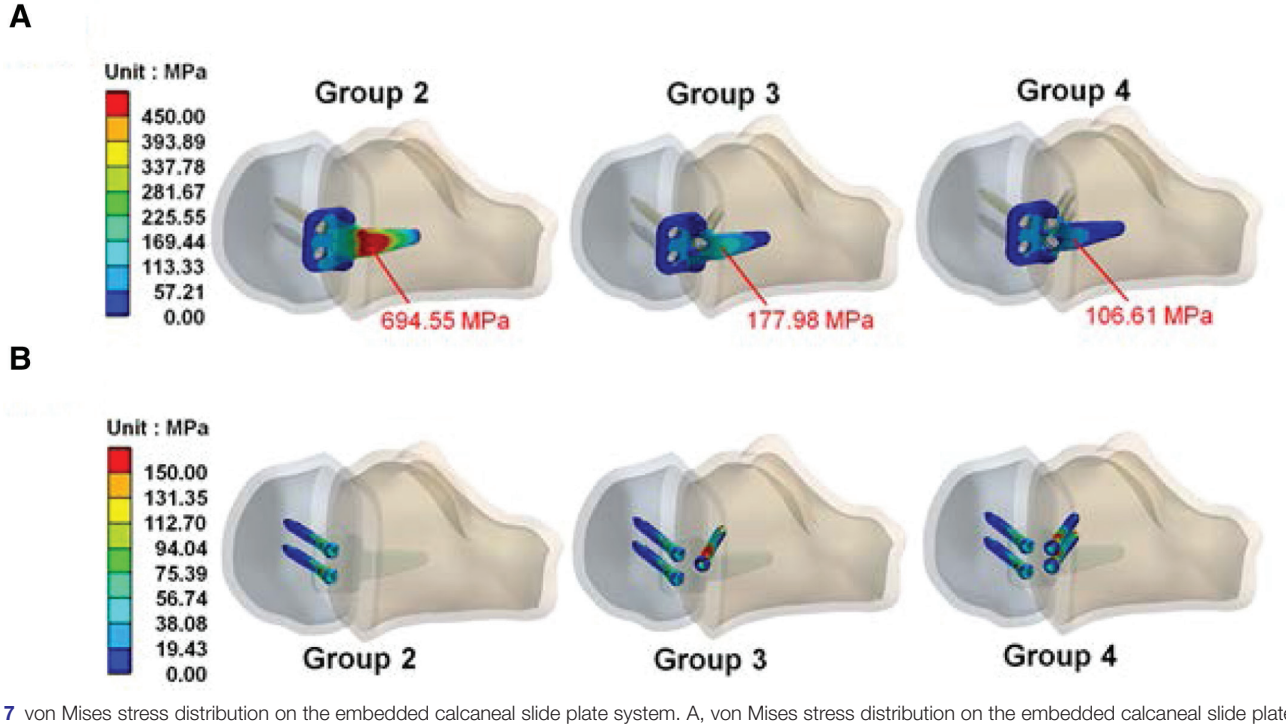

Fig. 7 von Mises stress distribution on the embedded calcaneal slide plate system. A, von Mises stress distribution on the embedded calcaneal slide plate. B, von Mises stress distribution on the fixation screws and diagonal screws of the embedded calcaneal slide plate.

Table 3

Maximum von Mises stress on the fixation screws and diagonal screws of the embedded calcaneal slide plate system

Screw	s1	s2	s3	s4	s5
Group 2	283.12 MPa	300.04 MPa	—	—	—
Group 3	270.75 MPa	289.93 MPa	2627.10 MPa	—	—
Group 4	278.22 MPa	283.09 MPa	—	1125.70 MPa	1369.30 MPa

—, not available.

non- and one-diagonal screw group. As expected, two-diagonal screw design on the calcaneal slide plate offered the best stability for MDCO fixation in three experiment groups even if no any design in this study can reach the stability of intact calcaneus (control group). Especially, no significance of differences in maximum force and stiffness were noted between one- and two-diagonal screw groups. Furthermore, significant rotation instability in group 2 under the preset load on the front of experimental specimens was found in DIC measurement (Fig. 10). These results suggested more than one-diagonal screw design

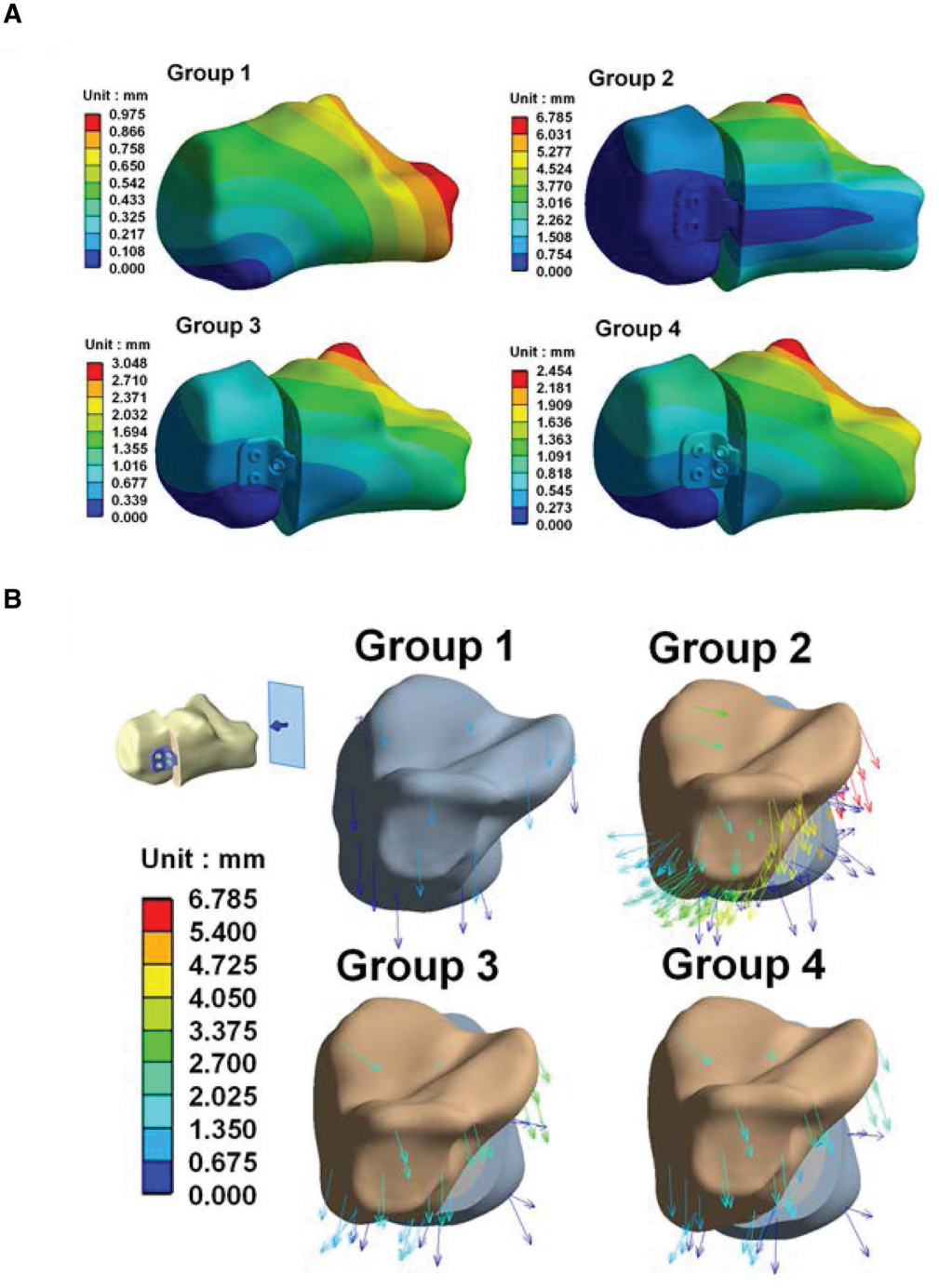

Fig. 8 The displacement of the calcaneus. A, Overall structural displacement of each group after loading with an external force. B, Direction of displacement in each group.

Table 4

The maximum force for 1.0 mm downward translation and stiffness tests

Observation index	Control	Non-diagonal screw	One-diagonal screw	Two-diagonal screws	*p*
Maximum force (N)					
Median (IQR)	27.56 (24.91-29.62)	4.12 (3.87-5.35)	8.73 (8.43-8.83)	10.59 (10.35-10.93)	0.009[b]
Stiffness (N/mm)					
Median (IQR)	24.27 (22.59-26.92)	3.34 (3.14-4.88)	6.81 (6.66-6.89)	9.21 (9.17-9.69)	0.009[b]

Kruskal-Wallis test.
[a]$p < 0.05$.
[b]$p < 0.01$.

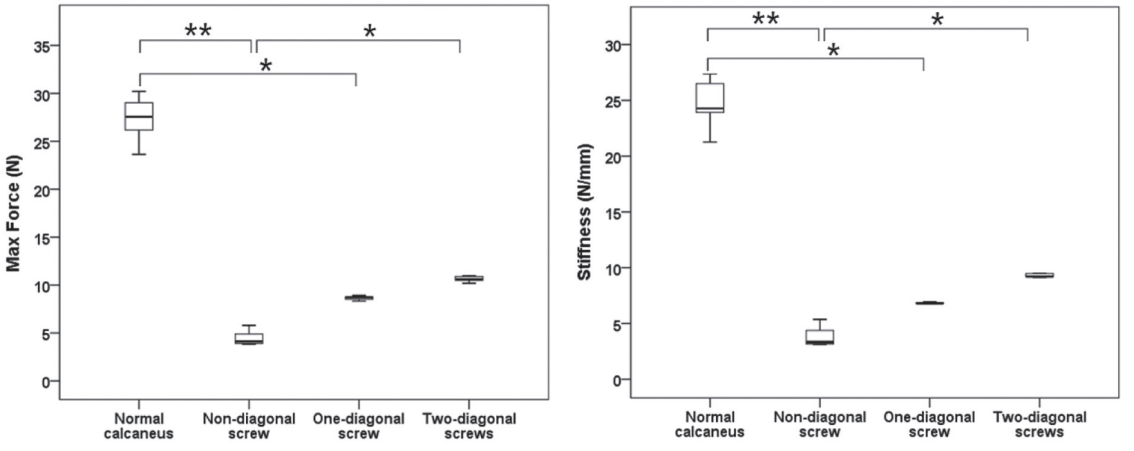

Fig. 9 The maximum force and stiffness of calcaneal modules implanted for MDCO in four groups, according to Kruskal-Wallis test (*$p < 0.05$, **$p < 0.01$). MDCO = medial displacement calcaneal osteotomy.

in the novel calcaneal slide plate is needed to supply better stability to avoid malunion or nonunion of the calcaneal osteotomy. The oblique compression "non-locking" screw was designed on the implant examined in this study. Hence, the distal osteotomy fragment of the calcaneus is fixed by the transverse screws of the implant (s1 and s2 in Fig. 2), the implanting conventional (non-locking) diagonal screws on the connecting area of the implant will apply the compression force proximally on the osteotomy site. Therefore, if there is no implantation of a diagonal screw on the implant trajectory to the proximal calcaneus, there will be no compression force on the osteotomy of MDCO. This factor might cause the delayed or nonunion of

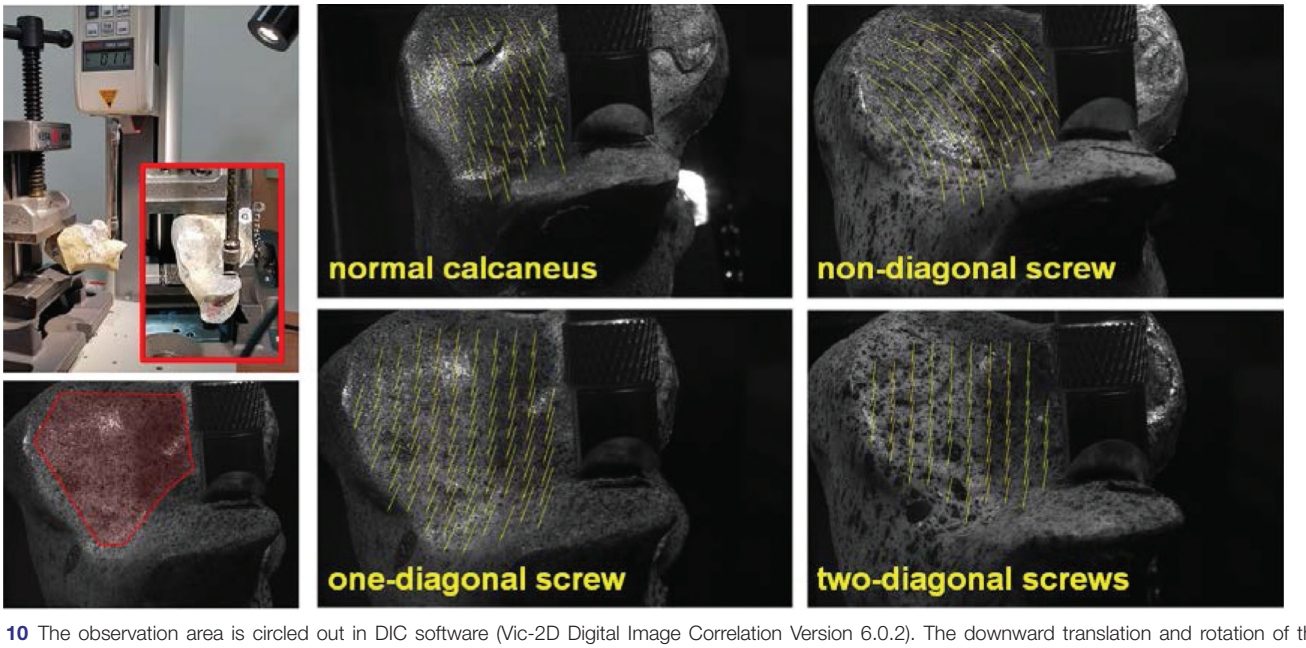

Fig. 10 The observation area is circled out in DIC software (Vic-2D Digital Image Correlation Version 6.0.2). The downward translation and rotation of the specimens with load progression from the top in DIC measurement. DIC = digital image correlation.

the osteotomy. We need more researches to explore the effect of different diagonal screw designs on the compression force at the interface of the osteotomy in the future. The results in vitro biomechanical testing were compatible to the finding of FEA.

The present study has some limitations. In our FEA, all material properties were assumed to be homogeneous, isotropic, and linearly elastic, as in previous studies,[21,23,25] in order to simplify the simulation and render the results of the study more comparable. However, the trends in the results of the main factors discussed remain unchanged. In addition, the computer models used in the present study were simplified. Although a complete model of the foot can be used to comprehensively evaluate the biomechanical situation of the entire foot, the structure of the foot is complex, making it impossible to observe the effects of the factors of interest in the study. Therefore, only the structure of the calcaneus was observed in the study. With these simplifications, there will be clearer trends and results for the topics of interest in the study despite the differences from the actual situation.

In the future, there are still many research topics related to Embedded Calcaneal Slide plate that are worth discussing. For example, the influence of different insertion angles of diagonal screws and the design of bone plates with different displacement distances of calcaneal nodule sawed. These are topics of great interest to orthopedic clinicians or plate designers. In this study, the results of this study can be used as a reference in further implant designs and mechanical studies so that patients with AAFD those who undergoing MDCO fixed by well-designed plate can obtain better surgical outcomes and medical quality.

In conclusion, this study, an embedded calcaneal slide plate suitable for implantation after MDCO was designed, and the biomechanical effects of design changes to the bone plate were investigated using FEA and biomechanical test. The results show that in order to avoid high stress concentration, increasing the number of diagonal screws can effectively reduce stress on the tapered blade tail and surrounding host bone, increase postoperative stability, and prevent calcaneal osteotomized bone rotation. We suggested more than one-diagonal screw design in the embedded calcaneal slide plate to offer better stability, especially by two. The results of this study provide a biomechanical reference to orthopedic surgeons and designers in the future design of calcaneal slide implants, which can reduce the failure rate after bone plate implantation after MDCO and improve the quality of medical care.

ACKNOWLEDGMENTS

We acknowledge the United States National Library of Medicine (NLM) and the Visible Human Project as the image source to build the finite element analysis model in this study. We would like to thank Taichung Veterans General Hospital (TCVGH-1085104B and TCVGH-HK1098002) in Taiwan and the 3D Printing Research and Development Group of Taichung Veterans General Hospital for helping us to build the simulation computer model of this study, and thank the Biostatistics Task Force of Taichung Veterans General Hospital and Mr Chen, Jun-Peng for statistical analysis.

REFERENCES

1. Aenumulapalli A, Kulkarni MM, Gandotra AR. Prevalence of flexible flat foot in adults: a cross-sectional study. *J Clin Diagn Res* 2017;**11**:AC17–20.
2. Abousayed MM, Alley MC, Shakked R, Rosenbaum AJ. Adult-acquired flatfoot deformity: etiology, diagnosis, and management. *JBJS Rev* 2017;**5**:e7.
3. Pita-Fernandez S, Gonzalez-Martin C, Alonso-Tajes F, Seoane-Pillado T, Pertega-Diaz S, Perez-Garcia S, et al. Flat foot in a random population and its impact on quality of life and functionality. *J Clin Diagn Res* 2017;**11**:LC22–7.
4. Kohls-Gatzoulis J, Woods B, Angel JC, Singh D. The prevalence of symptomatic posterior tibialis tendon dysfunction in women over the age of 40 in England. *Foot Ankle Surg* 2009;**15**:75–81.
5. Abousayed MM, Tartaglione JP, Rosenbaum AJ, Dipreta JA. Classifications in brief: Johnson and Strom classification of adult-acquired flatfoot deformity. *Clin Orthop Relat Res* 2016;**474**:588–93.
6. Van Gestel L, Van Bouwel S, Somville J. Surgical treatment of the adult acquired flexible flatfoot. *Acta Orthop Belg* 2015;**81**:172–83.
7. Parsons S, Naim S, Richards PJ, McBride D. Correction and prevention of deformity in type II tibialis posterior dysfunction. *Clin Orthop Relat Res* 2010;**468**:1025–32.
8. Myerson MS, Badekas A, Schon LC. Treatment of stage II posterior tibial tendon deficiency with flexor digitorum longus tendon transfer and calcaneal osteotomy. *Foot Ankle Int* 2004;**25**:445–50.
9. Burssens A, Barg A, van Ovost E, Van Oevelen A, Leenders T, Peiffer M, et al; Weightbearing CT International Study Group (WBCT ISG). The hind- and midfoot alignment computed after a medializing calcaneal osteotomy using a 3D weightbearing CT. *Int J Comput Assist Radiol Surg* 2019;**14**:1439–47.
10. Chan JY, Williams BR, Nair P, Young E, Sofka C, Deland JT, et al. The contribution of medializing calcaneal osteotomy on hindfoot alignment in the reconstruction of the stage II adult acquired flatfoot deformity. *Foot Ankle Int* 2013;**34**:159–66.
11. Schuh R, Gruber F, Wanivenhaus A, Hartig N, Windhager R, Trnka HJ. Flexor digitorum longus transfer and medial displacement calcaneal osteotomy for the treatment of stage II posterior tibial tendon dysfunction: kinematic and functional results of fifty one feet. *Int Orthop* 2013;**37**:1815–20.
12. Usuelli FG, Di Silvestri CA, D'Ambrosi R, Maccario C, Tan EW. Return to sport activities after medial displacement calcaneal osteotomy and flexor digitorum longus transfer. *Knee Surg Sports Traumatol Arthrosc* 2018;**26**:892–6.
13. Abbasian A, Zaidi R, Guha A, Goldberg A, Cullen N, Singh D. Comparison of three different fixation methods of calcaneal osteotomies. *Foot Ankle Int* 2013;**34**:420–5.
14. Saxena A, Patel R. Medial displacement calcaneal osteotomy: a comparison of screw versus locking plate fixation. *J Foot Ankle Surg* 2016;**55**:1164–8.
15. Müller C, Zippelius T, Strube P, Seeger JB, Brinkmann O, Matziolis G, et al. Calcaneal displacement osteotomies - less soft tissue irritation in lateral compression plate than screws. *Acta Chir Orthop Traumatol Cech* 2018;**85**:54–6.
16. Sayres SC, Gu Y, Kiernan S, DeSandis BA, Elliott AJ, O'Malley MJ. Comparison of rates of union and hardware removal between large and small cannulated screws for calcaneal osteotomy. *Foot Ankle Int* 2015;**36**:32–6.
17. Konan S, Meswania J, Blunn GW, Madhav RT, Oddy MJ. Mechanical stability of a locked step-plate versus single compression screw fixation for medial displacement calcaneal osteotomy. *Foot Ankle Int* 2012;**33**:669–74.
18. Coleman MM, Abousayed MM, Thompson JM, Bean BA, Guyton GP. Risk factors for complications associated with minimally invasive medial displacement calcaneal osteotomy. *Foot Ankle Int* 2021;**42**:121–31.
19. Haggerty EK, Chen S, Thordarson DB. Review of calcaneal osteotomies fixed with a calcaneal slide plate. *Foot Ankle Int* 2020;**41**:183–6.
20. Lucas DE, Simpson GA, Philbin TM. Comparing fixation used for calcaneal displacement osteotomies: a look at removal rates and cost. *Foot Ankle Spec* 2015;**8**:18–22.
21. Ouyang H, Deng Y, Xie P, Yang Y, Jiang B, Zeng C, et al. Biomechanical comparison of conventional and optimised locking plates for the fixation of intraarticular calcaneal fractures: a finite element analysis. *Comput Methods Biomech Biomed Engin* 2017;**20**:1339–49.
22. Pang QJ, Yu X, Guo ZH. The sustentaculum tali screw fixation for the treatment of Sanders type II calcaneal fracture: a finite element analysis. *Pak J Med Sci* 2014;**30**:1099–103.
23. Yu B, Chen WC, Lee PY, Lin KP, Lin KJ, Tsai CL, et al. Biomechanical comparison of conventional and anatomical calcaneal plates for the treatment of intraarticular calcaneal fractures - a finite element study. *Comput Methods Biomech Biomed Engin* 2016;**19**:1363–70.
24. Zhiwei Pan SH, Su Y, Qiao M, Zhang Q. Strain field measurements over 3000 °c using 3d-digital image correlation. *Opt Lasers Eng* 2020;**127**:105942.
25. Hung LK, Su KC, Lu WH, Lee CH. Biomechanical analysis of clavicle hook plate implantation with different hook angles in the acromioclavicular joint. *Int Orthop* 2017;**41**:1663–9.